Kirillov, S. V., & Semenkov, Y. P. (1982) *FEBS Lett. 148*, 235–238.
Kirillov, S. V., Makarov, E. M., & Semenkov, Y. P. (1983) *FEBS Lett. 157*, 91–94.
Lake, J. A. (1977) *Proc. Natl. Acad. Sci. U.S.A. 74*, 1903–1907.
Lill, R. (1981) Diplom Thesis, Universität München, München, West Germany.
Noll, H. (1966) *Science (Washington, D.C.) 151*, 1241–1245.
Odinzov, V. B., & Kirillov, S. V. (1978) *Nucleic Acids Res. 5*, 3871–3879.
Rappoport, S., & Lapidot, Y. (1974) *Methods Enzymol. 29*, 685–688.
Rheinberger, H.-J., & Nierhaus, K. H. (1980) *Biochem. Int. 1*, 297–303.
Rheinberger, H.-J., & Nierhaus, K. H. (1983) *Proc. Natl. Acad. Sci. U.S.A. 80*, 4213–4217.
Rheinberger, H.-J., Sternbach, H., & Nierhaus, K. H. (1981) *Proc. Natl. Acad. Sci. U.S.A. 78*, 5310–5314.
Rheinberger, H.-J., Schilling, S., & Nierhaus, K. H. (1983) *Eur. J. Biochem. 134*, 421–428.
Robertson, J. M., & Wintermeyer, W. (1981) *J. Mol. Biol. 151*, 57–79.
Schmitt, M., Möller, A., Riesner, D., & Gassen, H. G. (1981) *Eur. J. Biochem. 119*, 61–66.
Schmitt, M., Neugebauer, U., Bergmann, C., Gassen, H. G., & Riesner, D. (1982) *Eur. J. Biochem. 127*, 525–529.
Spirin, A. S. (1984) *FEBS Lett. 165*, 280–284.
Wagner, E. G. H., Jelenc, P. C., Ehrenberg, M., & Kurland, C. G. (1982) *Eur. J. Biochem. 122*, 193–197.
Watanabe, S. (1972) *J. Mol. Biol. 67*, 443–457.
Wettstein, F. O., & Noll, H. (1965) *J. Mol. Biol. 11*, 35–53.
Wintermeyer, W., & Robertson, J. M. (1982) *Biochemistry 21*, 2246–2252.

^{31}P and Two-Dimensional $^{31}P/^{1}H$ Correlated NMR Spectra of Duplex d(Ap[^{17}O]Gp[^{18}O]Cp[^{16}O]T) and Assignment of ^{31}P Signals in d(ApGpCpT)$_2$–Actinomycin D Complex†

David G. Gorenstein,* Kofen Lai, and Dinesh O. Shah

ABSTRACT: A solid-phase phosphoramidite method was used for the synthesis of unlabeled and phosphoryl-labeled d(Ap[^{17}O]Gp[^{18}O]Cp[^{16}O]T). The ability to label the phosphoryl oxygens of d(ApGpCpT) and thus assign the ^{31}P signals, combined with a two-dimensional $^{31}P/^{1}H$ chemical shift correlated NMR spectral technique, provided a novel means for the ready assignment of the H5′ and H3′ protons coupled to the phosphates. Phosphoryl labeling has also allowed us to assign the ^{31}P NMR signals in the actinomycin D–d(Ap[^{17}O]Gp[^{18}O]Cp[^{16}O]T)$_2$ duplex complex and confirm that the drug intercalates between the GpC stacked base pairs.

The interaction of drugs such as the antitumor antibiotic actinomycin D (Act D)[1] with nucleic acids is believed to perturb the conformation of the sugar–phosphate backbone. Indeed, much of the pharmacological activity of this and related drugs derives from their direct intercalation between stacked base pairs of the nucleic acids (Lown, 1977). When DNA structure is perturbed, these drugs may inhibit the synthesis of nucleic acids and interfere with cellular mitosis.

^{31}P NMR has been particularly useful in defining the intercalative mode of interaction (Muller & Crothers, 1968) of drugs such as actinomycin D with nucleic acids (Gorenstein & Goldfield 1984), since ^{31}P NMR chemical shifts in nucleic acids are a sensitive probe of P–O ester bond torsional angles (Gorenstein & Kar, 1975; Gorenstein, 1978, 1981, 1984). In one of the earliest demonstrations of ^{31}P spectral perturbations on drug binding, Patel (1974, 1976) and Reinhardt & Krugh (1977) showed that actinomycin D (Act D) shifted several phosphate diester signals up to 2.6 ppm downfield from the double-helical signals on binding to oligonucleotides containing dG-C base pairs. Thus, Patel (1976) showed that new ^{31}P signals appeared 1.6 and 2.6 ppm downfield in a d(CGCG)·Act D (2:1) complex.

These shifts are consistent with the Jain & Sobell (1972) model for these intercalated complexes: partial unwinding of a specific section of the double helix allows these planar heterocyclic drugs such as Act D to stack between two base pairs. X-ray studies of various intercalating drug–duplex complexes (Reddy et al., 1979; Shieh et al., 1980) suggest that the major backbone deformation of the nucleic acid on intercalation of the drug involves the C-5′–O-5′ torsional angle. However, in several complexes (Reddy et al., 1979) the P–O ester torsional angles (ω, ω') are altered from the normal B DNA ω, ω' conformation values of 290°, 290° (g^-,g^-; –gauche, –gauche) to values such as 273°, 323° and even 289.6°, 204.8° ($\sim g^-$,t) (Bhandary et al., 1984). Deshielding of the ^{31}P signals of up to 2.0 ppm has been calculated (Gorenstein & Kar, 1975; Gorenstein, 1983a,b, 1984) for torsional angle changes of this magnitude.

Since Act D is known to have a preference for G-C-rich DNA, it has been assumed that the site of intercalation is between two stacked d(G-C) base pairs (Remers, 1978). Unfortunately the one authenic X-ray structure of a Act D·d(G-C) complex (Takusagawa et al., 1982) does not contain

† From the Department of Chemistry, University of Illinois at Chicago, Chicago, Illinois 60680. *Received May 24, 1984.* This research was supported by NIH (GM-17575). Purchase of the IBM WP-200SY spectrometer was assisted by an NSF departmental equipment grant.

[1] Abbreviations: Act D, actinomycin D; COSY, ^{1}H two-dimensional J-correlation NMR; NOESY, ^{1}H two-dimensional NOE correlation NMR; EDTA, (ethylenedinitrilo)tetraacetic acid; FID, free induction decay; NMR, nuclear magnetic resonance; HPLC, high-pressure liquid chromatography; NOE, nuclear Overhauser effect; DSS, sodium 4,4-dimethyl-4-silapentanesulfonate; 2-D, two dimensional.

0006-2960/84/0423-6717$01.50/0

a double-helical structure. A proton NMR study by Patel et al. (1981) further strengthened this belief since Act D binding induced upfield shifts of the imino protons of cytosines in the duplex d(CGCGAATTCGCG)$_2$. Reid et al. (1983) have more recently used ^{1}H NMR nuclear Overhauser effects to support the G-C base pair intercalation site for Act D binding to duplex d(AGCT). Brown et al. (1984) have provided two-dimensional NOESY and COSY ^{1}H NMR spectra on an Act D complex of duplex d(ATGCAT).

Petersheim et al. (1984) have shown by ^{17}O labeling of the phosphoryl oxygens of d(CGCG) that the two ^{31}P signals in Patel's Act D study described above indeed belong to the two d(GC) phosphates. We now have used a similar labeling scheme to unambigously prove that the ^{31}P signals that are shifted downfield upon Act D binding to d(AGCT)$_2$ are associated with the d(GpC) phosphates and, by implication, that Act D does indeed only bind to the G-C stacked base pairs. We are also able to use a two-dimensional ^{31}P/^{1}H correlated NMR technique to assign the chemical shifts of the oligonucleotide 5′ and 3′ proton signals.

Experimental Procedures

Oligonucleotide Synthesis. A manual modification of the automated solid-phase phosphoramidite method (Applied Biosystems Manual, 1983; Caruthers, 1980; Tanaka & Letsinger, 1982) was used for the synthesis of unlabeled d(ApGpCpT) and the phosphoryl-labeled d(Ap[^{17}O]Gp[^{18}O]Cp[^{16}O]T) tetramers. For the unlabeled tetramer, 8 μmol of Applied Biosystems (dimethoxytrityl)deoxythymidine bound to porous silica (40 μmol of nucleotide/g of silica) was introduced to a specially constructed sintered glass filter unit. Detritylation was accomplished with 3% trichloroacetic acid in CH_2Cl_2. All nonaqueous solvents were rigorously dried and purified prior to use. An 8-fold excess of tetrazole-activated *N*-benzoyl-5′-(dimethoxytrityl)deoxycytidine was coupled to the free 5′-hydroxyl of the support-bound thymidine. Capping of any unreacted thymidine was accomplished with the addition of (dimethylamino)pyridine, acetic anhydride, and 2,6-lutidine. This protected phosphite dimer was oxidized with iodine/water in the presence of 2,6-lutidine. The cycle was repeated with the detritylation step, and addition of the appropriate protected (dimethoxytrityl)nucleoside phosphoramidite yielded the fully protected phosphate triester tetramer. Substitution of oxygen labeled water at the appropriate iodine/water oxidation step introduced the phosphoryl oxygen label. The total time required for the synthesis of the support-bound, fully protected (labeled or unlabeled) tetramer was 4 h, and the average coupling efficiency monitored by the amount of liberated dimethoxytritylcation was >95%.

The support-bound tetramer was treated with thiophenol and NH_4OH. The phosphate diester tetramer liberated from the support was purified by preparative C-18 reverse-phase HPLC (Alltech semiprep column). The partially protected tetranucleotide (>80% of the crude mixture was pure tetranucleotide) was collected and detritylated with 80% acetic acid, desalted on a Sephadex G-50-40 column with 10 mM triethylammonium bicarbonate as the eluent, and lyophilized. The purity of the tetramer was confirmed by HPLC (overall yield based on support-bound thymidine was 55–60%). d(pAGCT) was purchased from Collaborative Research. All oligonucleotides were treated with Chelex-100 (Bio-Rad) to remove paramagnetic metal ion impurities.

Actinomycin D was obtained from Sigma and used without further purification.

NMR Spectroscopy. The unlabeled tetramer (4.7 mg) was dissolved in 0.4 mL of 1 mM EDTA solution and adjusted to a pH meter reading of 7.0. For oxygen-labeled tetramer, 3.3 mg was used in the sample preparation. For the labeled tetramer–Act D sample, a weighed amount of Act D was added to yield a drug:tetramer ratio of 1:2.

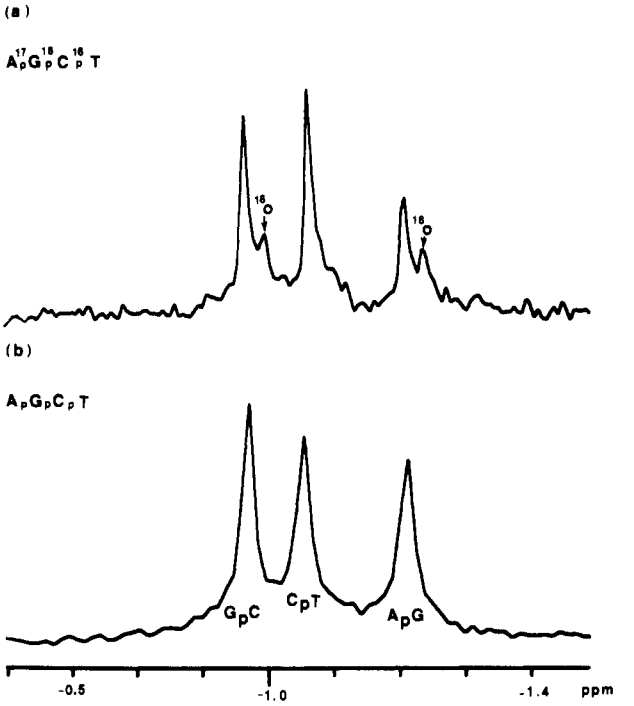

FIGURE 1: ^{31}P NMR spectrum of (a) d(Ap[^{17}O]Gp[^{18}O]T) and (b) d(ApGpCpT) at 81.0 MHz, 30 °C, in 1 mM EDTA, pH 7, D_2O.

High-field, Fourier transform ^{31}P NMR spectra were taken on IBM WP-200 SY or Nicolet NTC-200 NMR spectrometers (80.9-MHz ^{31}P) with proton noise, two-level decoupling, 56° pulses, 4K data points, and 1.4-s recycle time [see Gorenstein & Luxon (1979)]. At low field, spectra were recorded on a Bruker WP-80 spectrometer at 32.4 MHz (^{31}P) with 70° pulses, 8K data points, and 2.05-s recycle times. The spectra were broad-band ^{1}H decoupled.

All ^{31}P chemical shifts were referenced to 85% phosphoric acid in D_2O (0.00 ppm) at room temperature. Positive chemical shifts are downfield from phosphoric acid. ^{1}H chemical shifts are referenced to an HDO signal which is 4.66 ppm downfield from DSS. No magnetic susceptibility or temperature corrections were made to the ^{31}P chemical shifts reported in Figures 2 and 4.

Two-dimensional ^{31}P/^{1}H correlated NMR spectra used the Bruker heteonuclear shift-correlated 2-D NMR microprogram with the following parameters: X1 = 256, X2 = 2K, NS = 160, NE = 128, NI = 256, N2 = 2K; W1 = ±150 Hz, W2 = 1000 Hz, recycle delay 1.5 s, $t/2$ = 3 μs, τ_1 = 41.6 ms, τ_2 = 20.84 ms, phase cycling for quadrature detection. The FID's were Fourier transformed after treatment with a sine bell function in both domains and a Lorentz–Gauss function (LB = −3, GB = −0.3) in t_1.

Results

^{31}P NMR Spectra of d(AGCT) and d(pAGCT). Shown in Figure 1b is the spectrum of the unlabeled tetramer. The three ^{31}P signals have quite similar chemical shifts to the phosphate diester signals of an authentic sample of d(pApGpCpT) from Collaborative Research, and analysis of the ^{1}H NMR spectrum (discussed later) confirms the tetramer structure. The ^{31}P NMR spectrum of the phosphoryl oxygen labeled tetramer (Figure 1a) allows the immediate unambiguous identification of the signals. Thus, the upfield signal at −1.22 ppm is reduced

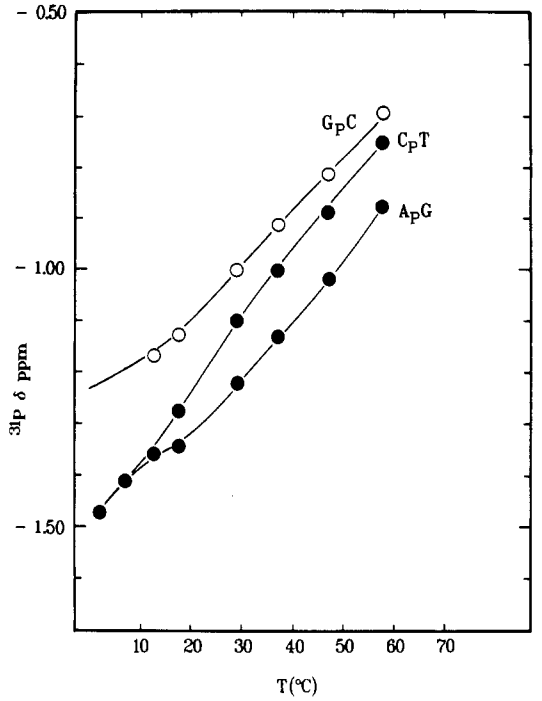

FIGURE 2: ^{31}P melting curves for d(pAGCT).

in intensity relative to the other main signals at −1.067 and −0.965 ppm. The ^{17}O directly bound to the phosphorus will broaden the high-resolution ^{31}P signal below detection due to the additional ^{17}O scalar relaxation of the second kind (Tsai, 1984), and only the ^{18}O-labeled and unlabeled signals will be observable. ^{18}O isotopic substitution perturbs the ^{31}P spectrum because this isotope is known to provide a small upfield isotopic shift on the ^{31}P signal (Cohn & Hu, 1978; Lowe & Sproat, 1978). Because ^{17}O was introduced into the ApG phosphate, the −1.22 ppm signal may be assigned to ApG. Since the ^{17}O water also is enriched with ^{18}O (51.1% ^{17}O, 39% ^{18}O; Monsanto Co.) an ^{18}O isotope shifted ^{31}P signal is also found 0.032 ppm upfield of the unlabeled ApG signal. Similarly the observation of the ^{18}O isotope shifted signal upfield of the −0.965 ppm signal identifies the Gp[^{18}O]C phosphate (note that the combined integrated intensity of the labeled and unlabeled GpC signals is the same as the integrated intensity of the *single* middle signal at −1.067 ppm, which thus is identified as the CpT phosphate). The isotopic level of ^{18}O enrichment in the water used for ^{18}O labeling was 49.3% ^{18}O and thus should have provided a 1:1 peak area ratio for the Gp[^{18}O]C and Gp[^{16}O]C peaks. As shown in Figure 1a, however, the ratio of the ^{18}O isotope shifted signal to the unlabeled GpC signal is only 0.20:1. Similarly while the ratio of the ^{17}O-labeled signal of ApG (obtained by difference) to the ^{18}O-labeled signal of ApG fits nicely with the original ^{17}O and ^{18}O enrichment of the water, the ^{16}O-labeled signal is much larger than would be expected on the basis of the 9.9% ^{16}O content of the ^{17}O water. Thus, as also noted by Seela et al. (1983), extraneous water (all ^{16}O of course) in the iodine oxidation step must still be present in our dried nonaqueous solvents. This does not present any problem, however, for our signal identification methodology.

The temperature dependence of the ^{31}P signals of d(pAGCT) is shown in Figure 2. We have assumed that the relative order of the ^{31}P signal assignments in d(AGCT) apply as well to d(pAGCT).

^{31}P NMR Spectra of Act D Labeled d(AGCT)$_2$. Shown in Figure 3 are ^{31}P NMR spectra of the Act D·d(Ap[^{17}O]Gp[^{18}O]Cp[^{16}O]T) complex (1:2) at various temperatures. As

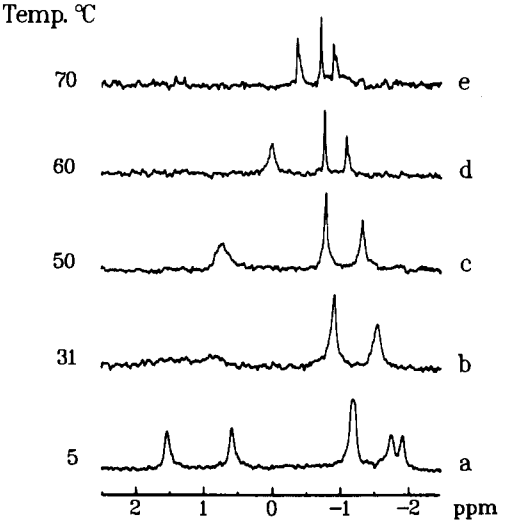

FIGURE 3: ^{31}P NMR spectra of Act D (1.5 mM) and d(Ap[^{17}O]-Gp[^{18}O]Cp[^{16}O]T) (3.0 mM) at 32.4 MHz and indicated temperatures.

previously observed (Patel, 1974; Reinhardt & Krugh, 1977; Petersheim et al., 1984) Act D produces large downfield shifts for two of the ^{31}P single phosphate signals upon complex formation. In Figure 3a, at 5 °C these two signals are shifted ~2.0 and 2.7 ppm downfield from the furthest upfield signal. Because of chemical exchange effect (see below) line broadening at low temperature, and additional signals, we cannot readily use the ^{17}O and ^{18}O labeling of the phosphates to identify the five ^{31}P signals in the low-temperature spectra. However, at high temperature (>60 °C; Figure 3d,c) where the drug complex is unstable, the expected ^{17}O and ^{18}O effects on the ^{31}P signals are observed. Thus, the central signal is sharp, with no multiplicity arising from ^{18}O-labeling, while the broad downfield signal (at −0.008 ppm, 60 °C) has the same intensity as the central signal at −0.618 ppm. Also at 60 °C, upfield signals at −0.879 and −0.907 ppm are observed. The −0.032 ppm difference between these two signals is consistent with an ^{18}O isotope shift, and the combined integrated intensity for these two upfield signals (and the broader upfield signal at lower temperatures) is only 80% of the −0.008 and −0.618 ppm signals and is thus readily assigned to the Ap[^{17}O]G phosphate. Since the −0.618 ppm signal shows no ^{18}O-isotopic multiplicity, it is assigned to the Cp[^{16}O]T phosphate, and therefore, the "broad" (6-Hz line width) downfield signal at −0.008 ppm must be assigned the Gp[^{18}O]C phosphate. Interestingly, although likely coincidentally, at high temperature the relative order of the ^{31}P signals of the tetranucleotide is the same as that of the free tetranucleotide ^{31}P signals.

By following the assigned ^{31}P signals to lower temperature in the presence of Act D (Figure 4), it is possible to assign the ^{31}P signals of the duplex–Act D complex. As demonstrated in the ^{1}H NMR study of d(AGCT)$_2$·Act D by Reid et al. (1983), at 30 °C the rate of chemical exchange between free duplex and complexed Act D is slow on the ^{1}H NMR chemical shift time scale (with intermediate chemical exchange observed above 35 °C). Similar behavior is observed in the ^{31}P NMR spectra of our study, although the ionic strength is different between the two studies. At low temperature (Figure 3a) five phosphates are in chemically distinct environments, and the binding of Act D must disrupt the 2-fold symmetry to the complex. At higher temperature the signals shift and coalesce (Figure 3c,d) as expected for an intermediate rate of chemical exchange. At higher temperature where the rate of chemical

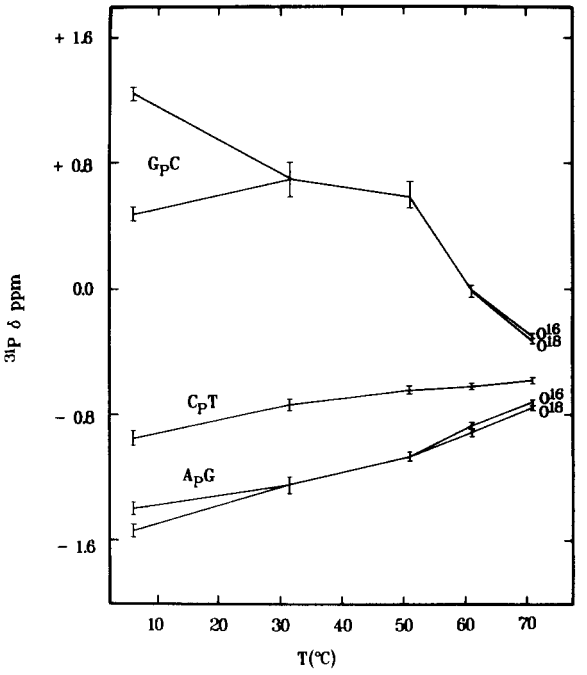

FIGURE 4: ^{31}P melting curves for signals in Figure 3 for Act D·d-(Ap[^{17}O]Gp[^{18}O]Cp[^{16}O]T) (1:2).

exchange is faster (and stability of the duplex is reduced), the ^{31}P signals sharpen. Assuming no unusual, discontinuous behavior for the ^{31}P chemical shifts as a function of temperature and the expected chemical exchange averaging of the signals (Pople et al., 1959), from Figure 4 and the high-temperature assignments, we have been able to assign the duplex–Act D ^{31}P signals. At 31 °C both of the d(GpC) phosphate signals in the drug complex shift 1.4–1.7 ppm downfield from the free duplex d(GpC) ^{31}P signals. The two d(CpT) phosphates are chemically indistinguishable in both the free duplex and drug complex, and the ^{31}P signals shift 0.3 ppm downfield upon complexation. The d(ApG) phosphate signals shift little at 31 °C upon complex formation, while at 5 °C (Figure 3a) separate signals for both phosphates can be seen (with a 0.2–0.3 ppm *upfield* shift in the complex).

2-D ^{31}P/^{1}H NMR. Pardi et al. (1983) have recently proven the power of 2-D NMR techniques in their assignment of the proton and phosphorus signals of the tetranucleotide d-(CpTpApG). As they point out, 2-D NMR methods inherently provide much greater spectral dispersion compared to normal one-dimensional NMR approaches where complex overlapping of the ^{1}H resonances make assignment of signals for even small oligonucleotides exceedingly difficult (Sarma, 1981; Cheng et al., 1982a,b). Since we have assigned the ^{31}P signals, we can through a 2-D ^{31}P/^{1}H chemical shift correlated spectrum (Bodenhausen & Freeman, 1977; Hutton, 1984) assign the H3′ and H5′ protons that are scalar coupled to the phosphates (contour plot, Figure 5). It is often difficult to observe the H3′ protons because they fall under the HDO peak, in the 1-D ^{1}H NMR spectrum. As shown in Figure 5, this HDO signal is eliminated in the greatly simplified ^{1}H spectrum derived from a projection of the 2-D spectrum–vertical ^{1}H axis spectrum. In addition H4′ protons often overlap with the H5′ protons, thus complicating the assignments. Since (except as noted below) the H4′ protons generally have a small 4-bond coupling to phosphorus (J < 1–2 Hz), they also do not appear in the 2-D ^{31}P/^{1}H 2-D correlated spectra optimized for 3-bond coupling (J > 5 Hz). The particular pulse sequence that generated the 2-D spectrum of Figure 5 eliminates ^{1}H coupling to the phosphorus signals as well as eliminates phosphorus coupling to the ^{1}H signals (although retaining all ^{1}H/^{1}H coupling).

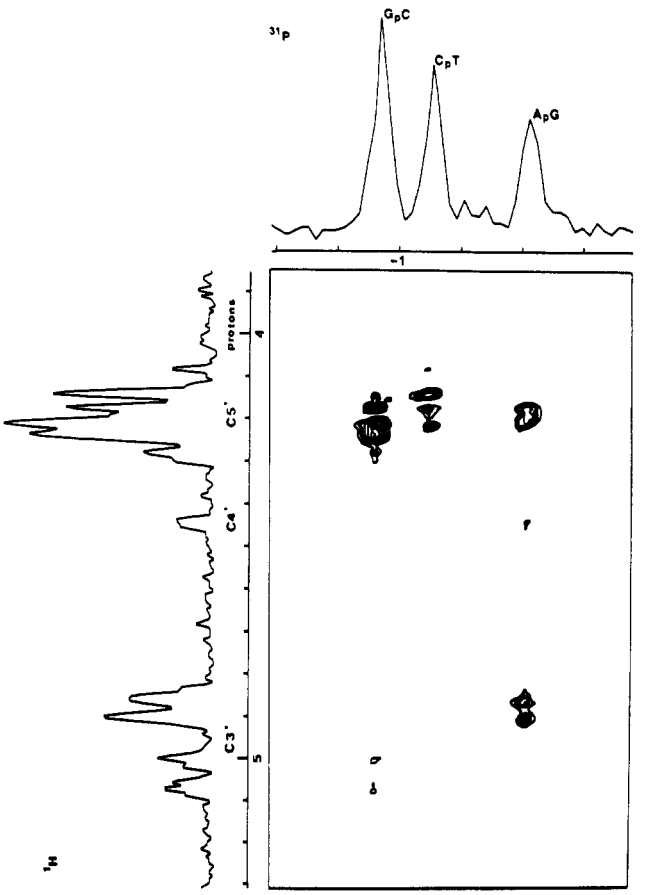

FIGURE 5: Two-dimensional ^{31}P/^{1}H chemical shift correlated contour plot of 0.01 M d(AGCT) in 0.4 mL of D_2O, at pH meter reading 7.0, 27 °C, and 1 mM EDTA at 200.13 MHz (^{1}H) on an IBM WP-200SY NMR spectrometer, spectral accumulation of 128 ^{31}P spectra (336 scans/FID), delay $1/(4J)$ = 0.03125 s (J = 8 Hz).

Table I: Chemical Shifts (ppm) of the Deoxyribose Ring Protons in d(AGCT) Complex, pD 7.0 and T = 27 °C

dinucleoside residue	chemical shift[a]		
	C-3′H	C-5′H_2[b]	C-4′H
GpC	5.04	4.23	
CpT	4.87	4.15	
ApG	4.89	4.17	4.34

[a] Relative to internal HDO peak at 4.66 ppm (relative to sodium 3-(trimethylsilyl)[2,2,3,3-$^{2}H_4$]propionate). [b] No stereochemical assignment of the two protons has been made.

Cross sections of the 2-D spectrum through each of the ^{31}P signals is shown in Figure 6. Because we have assigned the ^{31}P signals, the ^{31}P/^{1}H correlation means that we can unambiguously assign the H3′ and H5′ (5″) protons (except for H5′ of A and H3′ of T which are not coupled to a phosphate and thus their assignment cannot be made from the ^{31}P/^{1}H 2-D spectrum). In Table I we have compiled the chemical shifts of the assigned protons. In the 2-D experiment the delay time (Bax & Morris, 1981; Freeman & Morris, 1979) $1/(4J)$ corresponding to J values of 8 (Figure 5), 12, and 4 Hz (spectra not shown with considerably poorer S/N) have been used. Efficient transfer of the ^{1}H magnetization to the ^{31}P nucleus will only occur if these delays [$1/(4J)$] for multiplets and $1/(2J)$ for doublets) are comparable to the observed coupling constants ($J_{PH3'}$ and $J_{PH5'}$ vary from 5 to 10 Hz). Obviously some compromise in the delay time is required to provide the most efficient magnetization transfer and hence

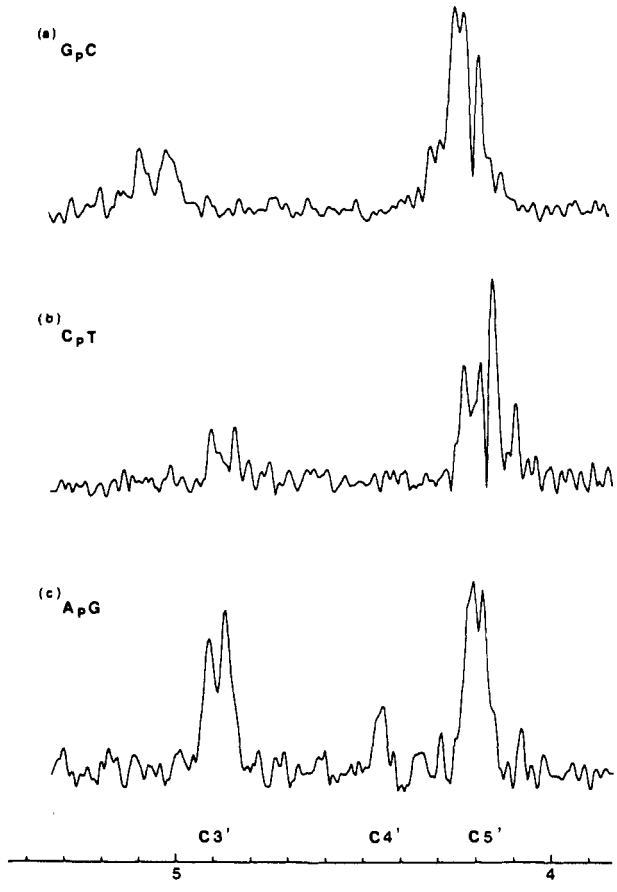

FIGURE 6: ^{1}H NMR cross sections of 2-D contour plot of Figure 5 for (a) GpC, (b) CpT, and (c) ApG phosphate signals.

signal intensity. By ^{1}H/^{1}H COSY (spectra not shown) with the *assigned* H3′ and H5′ protons we can also readily obtain through the ^{1}H/^{1}H J connectivity the chemical shifts of the other deoxyribose protons.

Discussion

^{31}P Chemical Shifts and Act D Binding to d(AGCT). Gorenstein & Kar (1975) have attempted to calculate the ^{31}P chemical shifts for a model phosphate diester in various geometries. These calculations revealed that ^{31}P chemical shifts should be dependent on P–O ester torsional angles (ω, ω') and O–P–O bond angles. These shift calculations suggested that a phosphate diester in a gauche,gauche (g,g)[2] conformation should have a ^{31}P chemical shift substantially upfield (by at least several ppm) from a phosphate diester in a gauche,trans (g,t) conformation [see also Prado et al. (1979)].

These insights into ^{31}P chemical shifts apply directly to the ^{31}P spectra of nucleic acid–drug complexes. As discussed in the introduction, Patel (1974) and Reinhardt & Krugh (1977) showed that Act D shifted several phosphate diester signals up to 2.6 ppm downfield from the double-helical signal upon binding to oligonucleotide duplexes containing d(GC) base pairs. These shifts are consistent with the Jain & Sobell (1972) model and recent X-ray studies (Reddy et al., 1979; Shieh et al., 1980; Bhandary et al., 1984) for these intercalated complexes: partial unwinding through a perturbation in the P–O ester and C-5′–O-5′ torsional angles of a specific section of the double helix allows these planar, heterocyclic drugs such as Act D to stack between two base pairs.

The 1.4–1.8 ppm downfield shifts which we observed for the d(GpC) phosphates of the ActD·d(AGCT)$_2$ complex are entirely consistent with the perturbation of the phosphate ester geometry via intercalation. The unperturbed helix signals for the d(ApG) and d(CpT) phosphates in this complex represent undisturbed phosphates in regions adjacent to the intercalation site. It also confirms that indeed Act D has a higher affinity for the d(GpC)·d(CpG) stacked base pairs than d(ApG)·d(TpC) stacked base pairs, as suggested earlier (Jain & Sobell, 1972; Patel, 1974, 1976; Reinhardt & Krugh, 1977). We have recently observed similar ^{31}P spectral changes upon intercalative binding of ethidium ion to double-helical poly(A)·oligo(U) (Goldfield et al., 1983; Lai et al., 1983; Gorenstein & Goldfield, 1984). These and other direct experimental tests of this torsional angle sensitivity to ^{31}P chemical shifts [Gorenstein et al., 1976, 1982; Gorenstein & Luxon, 1979; Gorenstein, 1981, 1983a,b, 1984; Chen & Cohen, 1984; see also Patel (1979a–d) and Gueron & Shulman (1975)] confirm that the ^{31}P signal of a phosphate diester monoanion in a gauche,gauche (g,g) conformation (as found in the helix state) should resonate several parts per million upfield from a diester in a nongauche conformation (as found in the random coil state). Thus, ^{31}P NMR spectroscopy can monitor the "helix–coil" transitions in single-stranded and double-stranded nucleic acids (Gorenstein et al., 1976, 1982). A large (0.7–1.3 ppm) downfield shift for a wide structural range of nucleic acids was observed when the temperature was raised. At low temperature, the nucleic acids will exist largely in a base-stacked, helical conformation with the phosphate ester predominantly in the gauche,gauche (g,g) conformation, while at higher temperatures, the nucleic acids will largely exist in random coil, unstacked conformations with the phosphate ester in an increased proportion of nongauche [i.e., gauche,trans (g,t) etc.] conformations [see, for example, reviews such as that of Ts'o (1975)].

As shown in Figure 2, d(pAGCT) behaves similarly, with deshielding of the ^{31}P signals at higher temperatures. In these low-salt conditions, even at low temperature a significant population of tetramers exists in the single-stranded state (Patel, 1976; Brown et al., 1984), and a sharp, cooperative-type melting curve is not expected or observed. However, a greater portion of the phosphates adopt the g,g conformation at lower temperature, giving rise to the upfield ^{31}P shift.

Act D will stabilize the double helix, and indeed as shown in Figure 4, on the basis of the ^{31}P melting curve for the complex, a melting temperature, T_m, of 55 °C can be estimated. In contrast to the noncooperative type melting curve shown in Figure 2, a sharper melting transition between 50 and 70 °C, indicative of a cooperative process, is observed for the DNA–drug complex (Figure 4).

Labeling Methodology. As described above, ^{31}P NMR can provide important structural and dynamic information on nucleic acids (Chen & Cohen, 1984; James, 1984; Gorenstein, 1984). In small oligonucleotides it is often possible to observe separate ^{31}P signals for each of the phosphate diesters, and thus, ^{31}P is potentially able to probe the conformational dynamics along the entire sugar–phosphate backbone. However, to obtain the greatest amount of information from the ^{31}P NMR spectra of oligonucleotides, it is imperative that a rapid and convenient method be available to label the phosphates and hence identify the ^{31}P signals. Recently both thiophosphoryl labeling (Eckstein, 1983; Stec, 1983) and ^{17}O phosphoryl labeling (Seela et al., 1983; Petersheim et al., 1984) have been introduced. Since thiophosphoryl labeling introduces

[2] We should mention at this time that for purposes of conveniently describing the torsional dependence of chemical shifts, we generally make no distinction between ROPO(R) torsional angles (ω) +60° (g^+) or –60° (g^-).

a new chiral center resulting in diastereomeric mixtures, and since sulfur substiution can perturb the structure of the nucleic acid (Eckstein, 1983), oxygen labeling is generally preferable. Labeling of the phosphoryl oxygen with ^{17}O is quite attractive since the additional ^{17}O scalar relaxation of the second kind will cause extensive line broadening of the ^{31}P NMR signal. Petersheim et al. (1984) have demonstrated the power of this technique in labeling one of the three phosphates in d(CGCG) with ^{17}O using the solution-phase phosphotriester methodology and showing the expected effect on the ^{31}P NMR spectrum. Since ^{18}O labeling of the phosphate is also possible (Cohn & Hu, 1978; Lowe & Sproat, 1978), a combination of ^{17}O and ^{18}O labeling makes it possible to unambiguously assign all three phosphate ^{31}P signals of the oligonucleotide tetramer d(AGCT) by site-specific introduction of the three different oxygen isotopes into the three different phosphate diesters. Most importantly, multimilligram quantities of labeled oligonucleotides may be readily obtained by a simple modification and scale-up of the solid-phase phosphoramidite oligonucleotide synthetic method (Caruthers, 1980; Tanaka & Letsinger, 1982). Perhaps even greater utilization of this phosphoryl oxygen labeling method will develop since rapid and convenient introduction of the labels requires no special capability other than the scaleup of the highly efficient solid-phase phosphoramidite synthesis as demonstrated here. It should also be noted that we have been able to identify all three ^{31}P signals from a double-labeled tetramer. Since we can introduce different ratios of the three oxygen isotopes at each cycle of the phosphite oxidation, it may be feasible to assign six or more phosphate signals in each preparation of a labeled hexamer or even larger oligomer.

2-D NMR. Proton NMR and in particular proton–proton and proton–phosphorus coupling constants and chemical shifts also provide important conformational and structural information on these molecules in solution (Sarma, 1981; Cheng et al., 1982a,b; Gorenstein, 1984), and unfortunately, it has not generally been possible to assign the nonexchangable protons on longer oligonucleotides by traditional selective decoupling one-dimensional NMR procedures, even at very high field. Pardi et al. (1983) required a combination of 2-D $^{31}P/^{1}H$ chemical shift correlated (Bodenhausen & Freeman, 1977; Hutton, 1984) and 2-D $^{1}H/^{1}H$ homonuclear correlated (COSY) (Aue et al., 1976) spectroscopy in order to make their assignments. Even at 500 MHz (^{1}H) the COSY spectra become very complex, and as a general method, it will become difficult to assign the signals for oligonucleotides larger than tetramers, although recent advances in 2-D NOE methodology look quite promising (Scheek et al., 1983). The NOESY spectral assignments, however, require an assumption that the DNA is in a regular B DNA geometry, which may not always be correct, especially in the case of DNA complexes. Our procedure, however, involves the simple chemical labeling of the phosphodiesters combined with analysis of the much less complex ^{31}P NMR spectrum and $^{1}H/^{31}P$ chemical shift correlated spectrum. In the latter, only those protons that are scalar coupled to the ^{31}P nucleus are observed in the 2-D spectrum (contour plot, Figure 5). Furthermore, there is every reason to believe that this methodology can be successfully applied to oligonucleotides much larger than the one described here.

Acknowledgments

The contributions of Bruce Luxon and Eugene DeRose to a portion of this work is much appreciated. We also greatly appreciate the advice of Drs. Wojciech Stec and Gerald Zon for the recommendation of the Applied Biosystems manual phosphoramidite oligonucleotide synthetic protocol and HPLC purification conditions.

Registry No. Act D, 50-76-0; d(ATGCAT)–Act D complex, 53360-01-3; d(Ap[^{17}O]Gp[^{18}O]Cp[^{16}O]T), 91126-91-9; d(GpC), 23405-83-6.

References

Aue, W. P., Bartholdi, E., & Ernst, R. R. (1976) *J. Chem. Phys. 64*, 2220.

Bax, A., & Morris, G. A. (1981) *J. Magn. Reson. 42*, 501.

Bhandary, K. K., Sakore, T. D., Sobell, H. M., King, D., & Gabbay, E. J. (1984) *J. Biomol. Struct. Dyn. 1*, 1195–1217.

Bodenhausen, G., & Freeman, R. (1977) *J. Magn. Reson. 25*, 471.

Brown, S. C., Mullis, K., Levenson, C., Shafer, R. H. (1984) *Biochemistry 23*, 403–408.

Caruthers, M. H. (1980) *Acc. Chem. Res. 13*, 155.

Chen, C.-W., & Cohen, J. S. (1984) in *^{31}P NMR: Principles and Applications* (Gorenstein, D. G., Ed.) Chapter 8, Academic Press, New York.

Cheng, D. M., Kan, L.-S., Leutzinger, E. E., Jayaraman, K., Miller, P. S., & Ts'o, P. O. P. (1982a) *Biochemistry 21*, 621.

Cheng, D. M., Kan, L.-S., Miller, P. S., Leutzinger, E. E., Ts'o, P. O. (1982b) *Biopolymers 21*, 697.

Cohn, M., & Hu, A. (1978) *Proc. Natl. Acad. Sci. U.S.A. 75*, 200.

Eckstein, F. (1983) *Ang. Chem., Int. Ed. Engl. 22*, 423.

Freeman, R., & Morris, G. A. (1974) *Bull. Magn. Reson. 1*, 5.

Goldfield, E. M., Luxon, B. A., Bowie, & Gorenstein, D. G. (1983) *Biochemistry 22*, 3336–3344.

Gorenstein, D. G. (1978) *Jerusalem Symp. Quantum Chem. Biochem. 11*, 1–15.

Gorenstein, D. G. (1981) *Annu. Rev. Biophys. Bioeng. 10*, 355–386.

Gorenstein, D. G. (1983a) *Prog. Nucl. Magn. Reson. Spectrosc. 16*, 1–98.

Gorenstein, D. G. (1983b) *Bull. Magn. Reson. 5*, 161–164.

Gorenstein, D. G. (1984) in *^{31}P NMR: Principles and Applications* (Gorenstein, D. G., Ed.) Chapter 1, Academic Press, New York.

Gorenstein, D. G., & Kar, D. (1975) *Biochem. Biophys. Res. Commun. 65*, 1073–1080.

Gorenstein, D. G., & Luxon, B. A. (1979) *Biochemistry 18*, 3796.

Gorenstein, D. G., & Goldfield, E. M. (1984) in *^{31}P NMR: Principles and Applications* (Gorenstein, D. G., Ed.) Chapter 9, Academic Press, New York.

Gorenstein, D. G., Findlay, J. B., Momii, R. K., Luxon, B. A., & Kar, D. (1976) *Biochemistry 15*, 3796.

Gorenstein, D. G., Luxon, B. A., Goldfield, E. M., Lai, K., & Vegeais, D. (1982) *Biochemistry 21*, 580–589.

Gueron, M., & Shulman, R. G. (1975) *Proc. Natl. Acad. Sci. U.S.A. 72*, 3482.

Hutton, W. C. (1984) in *^{31}P NMR: Principles and Applications* (Gorenstein, D. G., Ed.) Chapter 17, Academic Press, New York.

Jain, S. C., & Sobell, H. M. (1972) *J. Mol. Biol. 68*, 1.

James, T. (1984) in *^{31}P NMR: Principles and Applications* (Gorenstein, D. G., Ed.) Chapter 6, *Academic Press*, New York.

Lai, K., Goldfield, E. M., & Gorenstein, D. G. (1983) *Bull. Magn. Reson. 5*, 253.

Lowe, G., Sproat, B. S. (1978) *J. Chem. Soc., Chem. Commun.*, 565.

Lown, J. W. (1977) *Biorg. Chem. 3*, 95–121.
Muller, W., & Crothers, D. M. (1968) *J. Mol. Biol. 35*, 251–290.
Pardi, A., Walker, R., Rapoport, H., Wider, G., & Wüthrich, K. (1983) *J. Am. Chem. Soc. 105*, 1652.
Patel, D. J. (1974) *Biochemistry 13*, 2396.
Patel, D. J. (1976) *Biopolymers 15*, 533.
Patel, D. J. (1979a) *Acc. Chem. Res. 12*, 118.
Patel, D. J. (1979b) in *Stereodynamics of Molecular Systems*, pp 397–472, Pergamon Press, New York.
Patel, D. J. (1979c) *Eur. J. Biochem. 96*, 267.
Patel, D. J. (1979d) *Eur. J. Biochem. 99*, 369.
Patel, D. J., Kozlowski, S. A., Rice, J. A., Broka, C., & Itakura, K. (1981) *Proc. Natl. Acad. Sci. U.S.A. 78*, 7281–7284.
Petersheim, M., Mehdi, S., & Gerlt, J. A. (1984) *J. Am. Chem. Soc. 106*, 439.
Pople, J. A., Schneider, W. G., & Bernstein, H. J. (1959) *High Resolution Nuclear Magnetic Resonance*, Chapters 9 and 10, McGraw-Hill, New York.
Prado, F. R., Giessner-Prettre, C., Pullman, B., & Daudey, J.-P. (1979) *J. Am. Chem. Soc. 101*, 1737–1742.
Reddy, B. S., Seshadri, T. P., Sakore, T. D., & Sobell, H. M. (1979) *J. Mol. Biol. 135*, 787.
Reid, D. G., Salisbury, S. A., & Williams, D. H. (1983) *Biochemistry 22*, 1377–1385.
Reinhardt, C. G., & Krugh, T. R. (1977) *Biochemistry 16*, 2890.
Remers, W. A. (1978) in *The Chemistry of Antitumor Antibiotics*, Vol. 1, Wiley, New York.
Sarma, R. H., Dhingra, M. (1981) M. in *Topics in Nucleic Acid Structure* (Neidle, S., Ed.) Chapter 3, Wiley, New York.
Scheek, R. M., Russo, N., Boelens, R., Kaptein, R., & Van Boom, J. H. (1983) *J. Am. Chem. Soc. 105*, 2914–2916.
Seela, F., Ott, J., & Potter, B. V. C. (1983) *J. Am. Chem. Soc. 105*, 5879.
Shieh, H.-S., Berman, H. M., Debrow, M., & Neidle, S. (1980) *Nucleic Acids Res. 8*, 85.
Stec, W. J. (1983) *Acc. Chem. Res. 16*, 411.
Takusagawa, F., Dabrow, M., Neidle, S., & Berman, H. M. (1982) *Nature (London) 296*, 466–469.
Tanaka, T., & Letsinger, R. L. (1982) *Nucleic Acids Res. 10*, 3249.
Tsai, M. D. (1984) in *^{31}P NMR: Principles and Applications* (Gorenstein, D. G., Ed.) Chapter 6, Academic Press, New York.
Ts'o, P. O. P. (1975) *Basic Principles in Nucleic Acid Chemistry*, Vol. I and II, Academic Press, New York and London.

$2NH_2A{\cdot}T$ Helices in the Ribo- and Deoxypolynucleotide Series. Structural and Energetic Consequences of $2NH_2A$ Substitution†

Frank B. Howard* and H. Todd Miles*

ABSTRACT: Polynucleotide helices formed by the interaction of $(d2NH_2A)_n$, $(r2NH_2A)_n$, $(dT)_n$, and $(rT)_n$ have been prepared and their physical and spectroscopic properties examined. Thermal transitions, dependence of T_m on salt concentration, stoichiometry, phase diagrams, and calculated enthalpies are reported. UV, CD, and IR spectra are reported. All of the deoxy–deoxy helices containing $2NH_2A$ have positive CD first extrema near 290 nm and appear to have B-form structure. All the ribo–ribo or hybrid helices have negative first extrema in this region and appear to have A-form structure. Elevation of T_m by the 2-NH_2 group of $2NH_2A$ is much smaller in the deoxy than in the ribo series. We have applied an equation based on the electrostatic theory of Manning [Manning, G. S. (1972) *Bopolymers 11*, 937–949; Manning, G. S. (1978) *Q. Rev. Biophys. 11*, 179–246; Record, M. T., Anderson, C. F., & Lohman, T. M. (1978) *Q. Rev. Biophys. 11*, 103–178] to calculate ethalpies of the helix–coil transitions of the complexes reported here. These calculated enthalpies are larger for $2NH_2A{\cdot}T$ than for $A{\cdot}T$ helices, but the difference is much smaller in the deoxy than in the ribo series. We attribute these effects on T_m and ΔH in the deoxy series to loss of stabilization of the spine of hydration in B-form structures caused by interference of the 2-NH_2 group in the minor groove of the helix [Dickerson, R. E., Drew, H. R., Conner, B. N., Wing, R. M., Fratini, A. V., & Kopka, M. L. (1982) *Science (Washington, D.C.) 216*, 475–485]. Complete phase diagrams for all $2NH_2A$,T systems and some A,T systems are reported. The diagrams differ widely and can be placed in four groups according to the number of transitions each system possesses.

Introduction of a 2-NH_2 group into adenine residues of polynucleotides significantly perturbs their physical and spectroscopic properties, while maintaining base pairing specificity to uracil and thymine. A major chemical change occurs in the formation of three rather than two hydrogen bonds in AT and AU base pairs. These changes have been examined in detail in the ribopolynucleotide series (Howard et al., 1966, 1976; Muraoka et al., 1980). Preliminary studies in the deoxy series (Howard & Miles, 1983a,b; Howard et al., 1984) have shown striking contrasts from the ribo series in transition temperatures and circular dichroism (CD). In this paper we examine homopolymer systems containing $2NH_2A$ and T residues in the ribo and deoxy series with emphasis on the differences between the two. Relevance of the new data to the familiar three H-bond GC pair is also examined by using available data from the literature. The high transition temperatures of GC helices and the very stable self-structure of poly(G) have hindered or prevented direct observation of many

† From the Laboratory of Molecular Biology, National Institute of Arthritis, Diabetes, and Digestive and Kidney Diseases, National Institutes of Health, Bethesda, Maryland 20205. *Received June 21, 1984.*